Poly(ethylene terephthalate)/Attapulgite Nanocomposites: Preparation, Structure, and Properties

Xiayin Yao,[1] Xingyou Tian,[1,2] Xian Zhang,[1] Kang Zheng,[1] Jin Zheng,[1] Haobin Zhang,[2] Lin Chen,[1] Yong Li,[1,2] Ping Cui[1,2]

[1]*Key Laboratory of Materials Physics, Institute of Solid State Physics, Chinese Academy of Sciences, Hefei 230031, People's Republic of China*
[2]*Ningbo Institute of Material Technology & Engineering, Chinese Academy of Sciences, Ningbo 315040, People's Republic of China*

Received 27 November 2007; accepted 7 April 2008
DOI 10.1002/app.28501
Published online 16 June 2008 in Wiley InterScience (www.interscience.wiley.com).

ABSTRACT: In this study, poly(ethylene terephthalate) (PET)/attapulgite (AT) nanocomposites were prepared through the *in situ* polymerization of terephthalic acid, ethylene glycol, and AT, which was not premodified. By means of this new method, PET chains were successfully grafted onto the surface of AT, and this was confirmed by Fourier transform infrared spectroscopy, thermogravimetric analysis, and scanning electron microscopy. Transmission electron microscopy micrographs revealed that AT was well dispersed in the PET matrix. Differential scanning calorimetry and thermogravimetric analysis were used to investigate the thermal properties of the nanocomposites. The results suggested that the addition of AT could accelerate the crystallization rate and enhance the thermal stability of PET. Dynamic mechanical analysis results showed that the storage modulus of the PET/AT nanocomposites was greatly improved in comparison with that of pure PET. The tensile strength and modulus increased with increasing AT content. J Appl Polym Sci 110: 140–146, 2008

Key words: nanocomposites; polycondensation; structure-property relations

INTRODUCTION

In recent years, increased interest has been devoted to the synthesis of nanostructured polymer/inorganic nanocomposites because of their tremendously improved properties in comparison with conventional materials, such as electrical/magnetic properties, mechanical properties, thermal stability, gas-barrier properties, and fire retardancy.[1–3] One of the key points to the exceptional properties exhibited by polymer/inorganic nanocomposites is the homogeneous dispersion of the nanoscale particles in the polymer matrices. Many technologies have been developed to improve the distribution of particles and the bonding interaction between the particles and the matrix. Generally, polymer/inorganic nanocomposites can be prepared by *in situ* polymerization,[4–7] melt blending/extrusion,[8,9] or solution blending.[10,11] It has been proved that a homogeneous nanostructure can be formed in nanocomposites by an *in situ* polymerization process.

Poly(ethylene terephthalate) (PET) is a semicrystalline, low-cost thermoplastic polyester with good properties such as chemical resistance and thermal stability, and it has been widely used in the fields of fibers and nonfibers. However, disadvantages such as a low modulus and a low rate of crystallization limit its use in engineering applications. To overcome these shortcomings and improve its mechanical properties, many attempts have been made to prepare PET/inorganic nanocomposites. So far, many successful examples of PET/inorganic nanocomposites have been reported.[12–17]

Attapulgite (AT), a kind of natural, fibrous silicate clay with exchangeable cations and reactive —OH groups on its surface, has been widely used as an environmental absorbent, catalyst, carrier for pesticides and fertilizers, rheological control agent, and so on.[18–20] Because of its special morphology, surface properties, and low price, AT has drawn much attention in the preparation of polymer/AT nanocomposites. The polymer matrix includes polypropylene,[21] poly(acrylic acid),[22,23] polyamide,[24,25] epoxy resin,[26,27] and so on.[10,28–33] Li et al.[22] investigated the

Correspondence to: P. Cui (pcui@issp.ac.cn).
Contract grant sponsor: National Supporting Project; contract grant number: 2007BAE22B03.
Contract grant sponsor: Program of Ningbo Natural Science Foundation; contract grant number: 2006A610067.
Contract grant sponsor: Key Program of Ningbo Industrial Science and Technology; contract grant number: 2006B100062.

superabsorbent properties of a poly(acrylic acid)/AT composite and found that the composite exhibited excellent water absorbency and water retention under load. Lu et al.[27] treated AT with a simple organic modification to prepare epoxy nanocomposites; the results showed that the storage modulus and dimensional stability of the epoxy nanocomposites were improved significantly. However, in all cases, prior surface modification of AT was required, and up to now, only a few studies have been reported on the preparation of PET/AT nanocomposites.[34]

Herein we present a convenient *in situ* polymerization route for the preparation of PET/AT nanocomposites in which AT is not premodified. The monomers of PET, that is, terephthalic acid (TPA) and ethylene glycol (EG), are first reacted with the hydroxyl group on the AT surface, and then nanocomposites form by polycondensation. By means of this grafting-from method, AT is uniformly dispersed in the PET matrix. The greatest advantage of this study is that the thermal and mechanical properties of PET can be significantly improved with a very low loading of unmodified AT.

EXPERIMENTAL

Materials

AT was kindly supplied by Jiangsu Autobang International Co. (Jiangsu, China). TPA and antimony acetate (used as a catalyst) were obtained from Changzhou Huayuan Radics Co., Ltd. (Jiangsu, China). EG, phenol, tetrachloroethane, trifluoroacetic acid, chloroform, and absolute ethanol were purchased from Shanghai Chemical Reagent Corp. (Shanghai, China). All reagents were used without further purification.

Preparation of the pure PET and PET/AT nanocomposites

A given weight of AT was dispersed in deionized water and mixed with EG by ultrasonication for 10 min at room temperature. Then, the solution of AT and water/EG, TPA, and antimony acetate (250 ppm antimony with respect to the polymer) were mixed and introduced into a homemade reactor. The water was evaporated at 90°C under reduced pressure. After direct esterification and polycondensation, PET/AT nanocomposites were obtained. The details of polymerization can be found in our previous work.[4] Pure PET was synthesized under the same reaction conditions mentioned previously in the absence of AT. The PET/AT nanocomposites with 0.5, 1, and 2 wt % AT were labeled PET/0.5AT, PET/1AT, and PET/2AT, respectively.

To isolate the PET-grafted AT nanocomposites from the PET/AT nanocomposites containing ungrafted PET, the PET/AT nanocomposites were dispersed in a mixture of phenol and tetrachloroethane (30/50 w/w). There was no insoluble portion found, and the complete dispersion was obtained. The dispersion was centrifuged at 10,000 rpm until the AT was precipitated. The supernatant solutions were added dropwise to a 10–15-fold excess of methanol. Then, the precipitated AT was repeatedly redispersed in the aforementioned mixture of solvents and separated again by centrifugation. This dissolution–precipitation procedure was repeated until no more precipitate formed when the supernatant liquid was added dropwise to methanol, and this indicated that no ungrafted and adsorbed PET could be removed. The resulting solid materials, that is, PET-grafted AT nanocomposites, were washed extensively with absolute ethanol to remove the solvent and dried to a constant weight at 80°C *in vacuo*. The PET-grafted AT nanocomposites, separated from the PET/0.5AT, PET/1AT, and PET/2AT nanocomposites, were labeled PET-grafted 0.5AT, PET-grafted 1AT, and PET-grafted 2AT, respectively.

Characterization

Fourier transform infrared (FTIR) spectra of AT and PET-grafted AT nanocomposites were recorded at the ambient temperature on a Nicolet Magna-IR 750 spectrometer (Nicolet Instrument Co., USA) over the range of 400–4000 cm^{-1}. The sample was ground with dried potassium bromide (KBr) powder and compressed into a disc and then was subjected to analysis.

Transmission electron microscopy (TEM) images of PET/AT nanocomposites were obtained on a JEOL 100CX II transmission electron microscope (JEOL Ltd., Japan) operated at 120 kV. The nanocomposites samples were cut into approximately 80–100-nm-thick slices with an ultramicrotome with a diamond knife.

The morphology of AT and PET-grafted AT nanocomposites was observed with a Sirion 200 field emission scanning electron microscope (FEI Co., USA). AT and PET-grafted AT nanocomposites were fully dispersed in ethanol and a mixture of trifluoroacetic acid and chloroform (1/20 v/v), respectively. After the evaporation of the solvents, the samples were coated with a thin layer of gold before the scanning electron microscopy (SEM) examination.

Differential scanning calorimetry (DSC) measurements were performed with a PerkinElmer Pyris Diamond differential scanning calorimeter (Pyris software, version 6.5) (Perkin Elmer, Inc., USA). Under a nitrogen atmosphere, the samples (4–5 mg) of pure PET and PET/AT nanocomposites were first heated to 270°C at a heating rate of 10°C/min and then annealed at this temperature for 5 min to

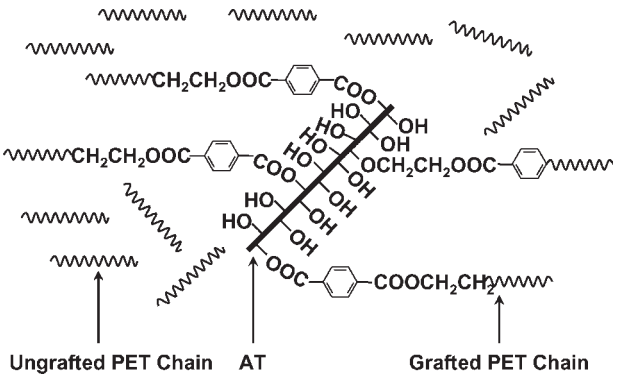

Scheme 1 Sketch map of the structure of the PET/AT nanocomposites.

remove the thermal history before cooling at 10°C/min.

Thermogravimetric analysis (TGA) was performed with a PerkinElmer Pyris-1 thermal analyzer (Perkin Elmer, Inc., USA). The samples of pure PET and PET/AT nanocomposites were heated to 750°C at a rate of 10°C/min under a nitrogen atmosphere, whereas AT and PET-grafted AT nanocomposites were heated to 750°C at a rate of 10°C/min in air.

Dynamic mechanical analysis (DMA) was performed on the samples of pure PET and PET/AT nanocomposites with a PerkinElmer Diamond dynamic mechanical analyzer (Perkin Elmer, Inc., USA). All samples were cut out to the size of 60 × 5.5 × 2.6 mm^3 from compression-molded plaques. The tests were carried out in a bending mode over a temperature range of −140 to 150°C at 1 Hz and a heating rate of 2°C/min.

For the intrinsic viscosity measurements, a 250 ± 5 mg sample was introduced into a 100-mL mixture of phenol and tetrachloroethane (60/40 w/w), and the measurements were performed with an Ubbelohde viscometer. Tensile testing was carried out on a universal tester (model CMT4204, SANS Test Machine Co., Ltd., Shenzhen, China) according to ASTM D 638.

RESULTS AND DISCUSSION

Structure and morphology

It is well known that the dispersion of a filler in a polymer matrix and the interfacial interaction between them significantly affect the properties of the composites. As the fillers are difficult to disperse uniformly in polymer matrices because of agglomeration and immiscibility between the filler and polymer matrix, many efforts have been made to surface-modify the filler to improve its adhesion with the polymer matrix. However, in this study, AT was first dispersed in EG to form PET/AT nanocomposites through direct esterification and polycondensation without any surface modifier. The obtained samples had intrinsic viscosities ranging from 0.671 (pure PET) to 0.606, 0.615, and 0.623 dL/g (PET/AT with AT weight contents of 0.5, 1, and 2%, respectively). A sketch map of the structure of the PET/AT nanocomposites is shown in Scheme 1. As AT and EG are all hydrophilic, AT can easily be dispersed in a mixture of water and EG by ultrasonication. During the esterification process, TPA and EG can react with the hydroxyl group on the AT surface, and this will improve the compatibility of AT and PET greatly. This assertion can be confirmed by FTIR spectroscopy, TGA, SEM, and TEM examination.

The FTIR spectra of pure PET, AT, and PET-grafted AT nanocomposites are shown in Figure 1. Comparing the spectra of PET-grafted AT nanocomposites [Fig. 1(c–e)] with the spectra of pure PET [Fig. 1(a)] and AT [Fig. 1(b)], we find that the appearance of both absorption bands at 1724 and 1030 cm^{-1}, attributed to the characteristic band of C=O stretching of the ester carbonyl group[35] and the stretching vibration of the Si—OH bond,[34] proves the existence of PET and AT and indicates the interaction between them. The weakened absorption band of Si—OH [Fig. 1(c–e)], compared with the spectra of AT [Fig. 1(b)], gives direct evidence for the reaction between AT and monomers of PET, that is, TPA and EG. It can be concluded that some PET molecules are grafted onto AT through chemical bonding rather than physical absorption. A similar reaction was reported by Bikiaris et al.[35] for PET/silica nanocomposites.

The amount of PET grafted onto the AT surface was determined by TGA at the heating rate of 10°C/min from 100 to 750°C in air. The repeated cycles of a dissolution–precipitation procedure were

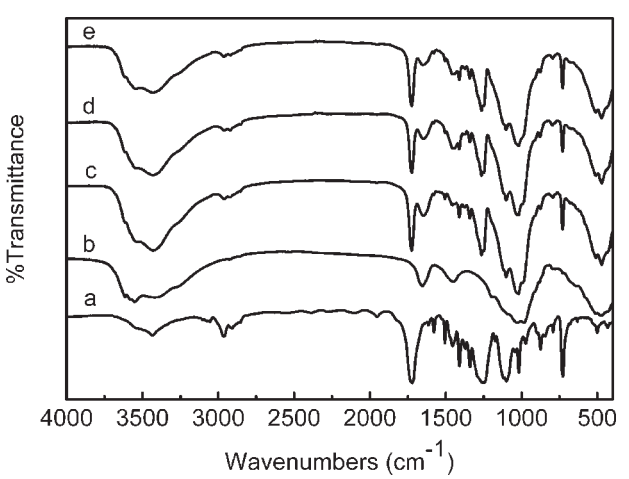

Figure 1 FTIR spectra for (a) pure PET, (b) AT, (c) the PET-grafted 0.5AT nanocomposite, (d) the PET-grafted 1AT nanocomposite, and (e) the PET-grafted 2AT nanocomposite.

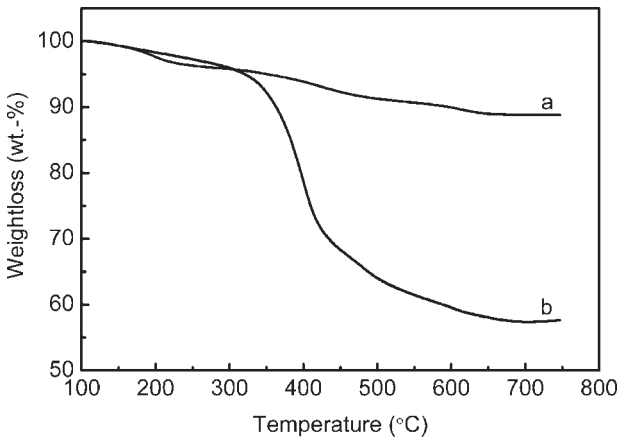

Figure 2 TGA curves for (a) AT and (b) the PET-grafted 1AT nanocomposite.

employed to remove ungrafted and adsorbed PET. Figure 2 shows the weight-loss curves for the AT and PET-grafted 1AT nanocomposite. The fraction of grafted PET was 31.3 wt % with respect to the weight of ungrafted AT.

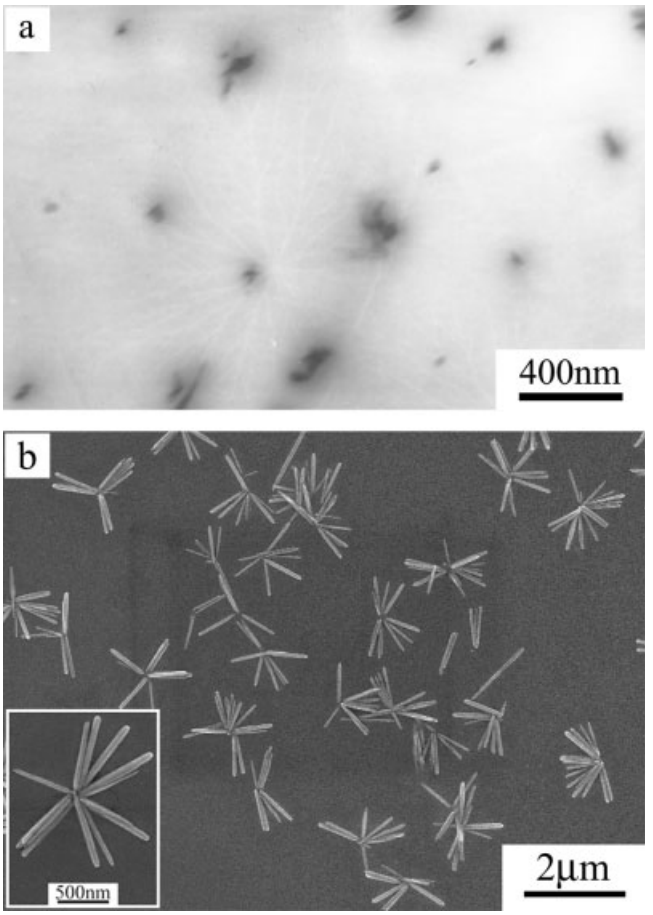

Figure 3 (a) TEM micrograph of the PET/1AT nanocomposite and (b) SEM micrograph of the PET-grafted 1AT nanocomposite (the insert is PET-grafted 1AT nanocomposite at high magnifying power).

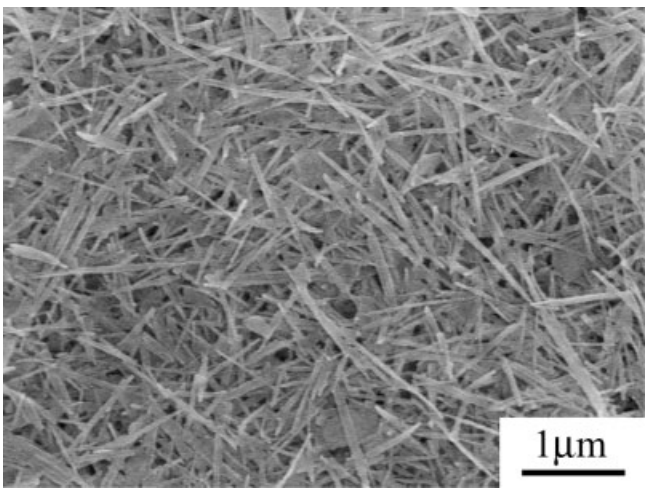

Figure 4 SEM micrograph of the as-received AT.

The surface grafting of a polymer onto inorganic fillers is known to be very effective at improving the dispersability in polymer matrices.[36] TEM was used to examine the quality of the dispersion of AT in PET. Figure 3(a) shows the TEM micrograph of the PET/1AT nanocomposite. AT was well dispersed in the PET matrix. The morphology of the PET-grafted 1AT nanocomposite was observed directly by SEM examination, as shown in Figure 3(b). It is surprising to find that the PET-grafted 1AT nanocomposite consisted of separated single rods. However, the diameters of the PET-grafted 1AT nanocomposite did not change significantly in comparison with the as-received AT (Fig. 4). It can be concluded that the polymerization of PET on the surface of AT improves the dispersion of AT in the PET matrix and the interfacial adhesion between them, and this would no doubt improve the performance of PET.

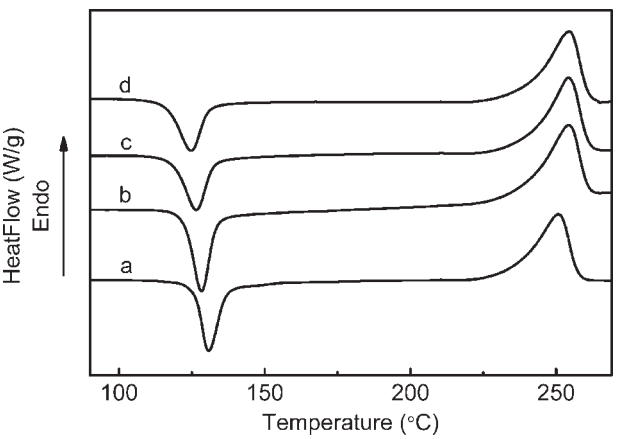

Figure 5 Heating measurement of the DSC trace for (a) pure PET, (b) the PET/0.5AT nanocomposite, (c) the PET/1AT nanocomposite, and (d) the PET/2AT nanocomposite.

TABLE I
Thermal Properties of the Pure PET and PET/AT Nanocomposites

Sample	T_{cc} (°C)	T_m (°C)	ΔH_m (°C)	T_{mc} (°C)	$T_m - T_{mc}$ (°C)	T_d (°C)	Residue at 700°C (wt %)
Pure PET	130.77	250.79	40.91	194.62	56.17	383.92	13.9
PET/0.5AT	128.33	254.19	43.07	208.87	45.32	385.62	14.5
PET/1AT	126.42	254.05	43.69	209.05	45.00	387.26	16.1
PET/2AT	124.72	254.44	44.38	211.79	42.65	390.04	18.2

Thermal properties

Many researchers have reported that the addition of a filler to a polymer matrix can increase the crystallization rate of the polymer.[4,37,38] In this study, we have found that PET filled with AT results in somewhat of a change in the thermal properties. Figure 5 shows the DSC heating curves of pure PET and PET/AT nanocomposites. The cold crystallization temperature (T_{cc}), melting point (T_m), melting enthalpy (ΔH_m), crystallization temperature during melt cooling (T_{mc}), and degree of supercooling ($T_m - T_{mc}$) are listed in Table I. The T_{mc} values of the PET/AT nanocomposites are higher than that of pure PET, and this indicates that AT could act as heterogeneous nuclei of PET. Furthermore, in comparison with the pure PET, the values of ΔH_m for the PET/AT nanocomposites are larger, and this means that the crystallinity of PET increases with the addition of AT.

The DSC cooling curves of pure PET and PET/AT nanocomposites are shown in Figure 6. The curves of all samples show a crystallization exothermic peak, but the crystallization peak width and crystallization temperature have changed greatly. The width of the half-height of the crystallization peak for the PET/AT nanocomposites is narrower by about 8°C than that of pure PET. Generally, the degree of supercooling is the thermodynamic drive near T_m;[7] that is, the smaller the degree of supercooling is, the higher the crystallizability is. Filling PET with AT decreases the degree of supercooling by 10.85–13.52°C in comparison with pure PET, as shown in Table I. It can be concluded from these results that AT could play a role as a nucleating agent in PET crystallization and lead to an acceleration of crystallization.

Generally, the introduction of an inorganic filler into polymer matrices can improve the thermal stability of the polymer.[7,13,39] In Figure 7, the curves of pure PET and PET/AT nanocomposites at the heating rate of 10°C/min in a nitrogen atmosphere are shown. The onset temperature of thermal decomposition (T_d) of the PET/AT nanocomposites changes from 385.62 to 390.04°C with the AT content increasing from 0.5 to 2 wt %, whereas the T_d value of pure PET is 383.92°C. In addition, the residue content of the PET/AT nanocomposites at 700°C is larger than that of PET, and the greater the AT content is, the larger the residue content is. These results show that PET/AT nanocomposites possess improved thermal stability in comparison with pure PET, and this can be attributed to the strong interaction between the AT and PET matrix.

Mechanical properties

The mechanical properties of materials depend on their structure. DMA is a powerful tool for studying

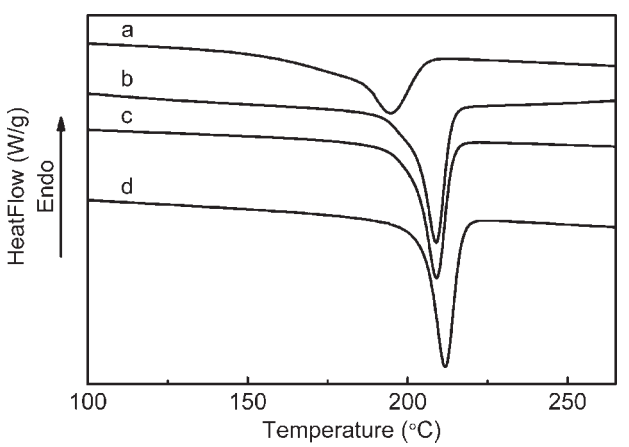

Figure 6 Cooling measurement of DSC trace for (a) pure PET, (b) the PET/0.5AT nanocomposite, (c) the PET/1AT nanocomposite, and (d) the PET/2AT nanocomposite.

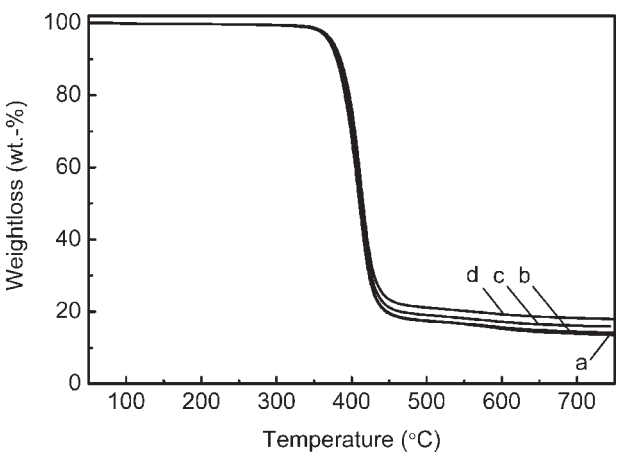

Figure 7 TGA curves for (a) pure PET, (b) the PET/0.5AT nanocomposite, (c) the PET/1AT nanocomposite, and (d) the PET/2AT nanocomposite.

the mechanical properties and molecular-scale motion of polymers under small-strain conditions. Generally, the damping (tan δ) curve of PET exhibits three relaxation peaks around 100 (α), −70 (β), and −230°C (γ).[40] Among the three relaxation peaks, the α- and β-relaxations in PET have been widely studied.[41–44] In this work, we focus on the α-relaxation in PET, which is associated with the glass-transition temperature (T_g). Many reports have demonstrated the effects of grafting and chain immobilization on T_g of a polymer.[45,46] Figure 8 shows the bending storage modulus (E') as well as α- and β-relaxations for the pure PET and PET/AT nanocomposites. T_g, defined as the peak temperature of the α-relaxation, can be extracted from the tan δ/temperature curve, and the results are summarized in Table II. T_g of the PET/AT nanocomposites is higher than that of pure PET. The shift of T_g is due to the grafting of PET chains onto the surface of AT, which reduces the mobility of the chains. The result indicates good interfacial adhesion between PET and AT. Similar phenomena have been reported on polyamide 6/AT nanocomposites[24,25] and epoxy resin/AT nanocomposites.[27]

The E' values of pure PET and PET/AT nanocomposites at 60 and 100°C, derived from Figure 8, are also presented in Table II. It can be seen clearly that PET/AT nanocomposites have higher E' values than pure PET over the whole temperature range. Moreover, the E' value of the PET/AT nanocomposites increases with increasing AT content. Compared with that of the pure PET, the E' value of the PET/2AT nanocomposite is increased by 40.0% at 60°C and by 76.4% at 100°C. This significant improvement in the E' values of PET/AT nanocomposites are attributed both to the covalent link between the AT and PET matrix and the well-dispersed AT in the PET matrix.

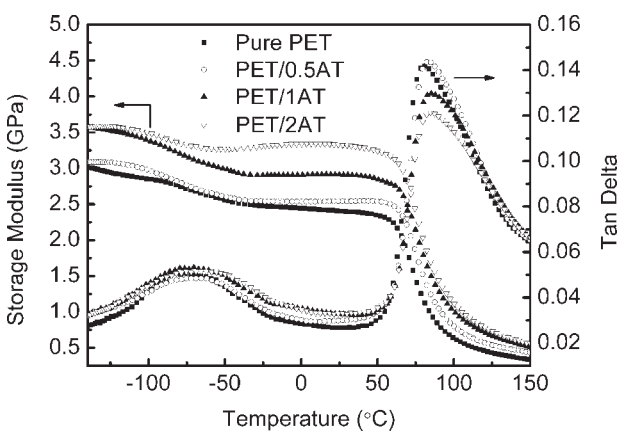

Figure 8 E' and tan δ of pure PET and the PET/AT nanocomposite as a function of temperature with a heating rate of 2°C/min and a frequency of 1 Hz on the basis of bending-mode DMA measurements.

TABLE II
T_g and Mechanical Properties of the Pure PET and PET/AT Nanocomposites

Sample	T_g (°C)	E' (GPa) 60°C	E' (GPa) 100°C	Tensile strength (MPa)	Tensile modulus (GPa)
Pure PET	81.1	2.248	0.635	55.82	2.624
PET/0.5AT	82.2	2.483	0.802	59.95	2.791
PET/1AT	85.2	2.772	1.010	60.95	3.311
PET/2AT	84.9	3.145	1.120	61.35	3.803

The tensile results for the pure PET and PET/AT nanocomposites are also listed in Table II. Both the tensile strength and tensile modulus increase with the addition of AT. The tensile modulus for the PET/2AT nanocomposite exhibits a 45% increment in comparison with that of the pure PET.

CONCLUSIONS

We have developed a convenient method for preparing PET/AT nanocomposites in which AT is not premodified. The nanocomposites were synthesized by the *in situ* polymerization of TPA, EG, and AT. PET chains were successfully grafted onto the surface of AT, and this improved the interfacial adhesion between the AT and PET matrix. The uniform dispersion of AT in the PET matrix had important effects on the thermal and mechanical properties of PET. The existence of AT could lead to an acceleration of crystallization and enhance the thermal stability of PET. Moreover, the introduction of AT could enhance the storage modulus and make T_g of PET shift to a higher temperature. The tensile strength and modulus were also improved significantly.

References

1. Pyun, J.; Kowalewski, T.; Matyjaszewski, K. Macromol Rapid Commun 2003, 24, 1043.
2. Kickelbick, G. Prog Polym Sci 2003, 28, 83.
3. MacLachlan, M. J.; Manners, I.; Ozin, G. A. Adv Mater 2000, 12, 675.
4. Liu, W. T.; Tian, X. Y.; Cui, P.; Li, Y.; Zheng, K.; Yang, Y. J Appl Polym Sci 2004, 91, 1229.
5. Chang, J. H.; An, Y. U.; Kim, S. J.; Im, S. Polymer 2003, 44, 5655.
6. Imai, Y.; Nishimura, S.; Abe, E.; Tateyama, H.; Abiko, A.; Yamaguchi, A.; Aoyama, T.; Taguchi, H. Chem Mater 2002, 14, 477.
7. Qu, M. H.; Wang, Y. Z.; Wang, C.; Ge, X. G.; Wang, D. Y.; Zhou, Q. Eur Polym J 2005, 41, 2569.
8. Alexandre, M.; Dubois, P. Mater Sci Eng R-Rep 2000, 28, 1.
9. Giannelis, E. P. Adv Mater 1996, 8, 29.
10. Peng, Z. Q.; Chen, D. J. J Polym Sci Part B: Polym Phys 2006, 44, 1995.
11. Jeon, H. G.; Jung, H. T.; Lee, S. W.; Hudson, S. D. Polym Bull 1998, 41, 107.
12. Yang, Y. Z.; Gu, H. C. J Appl Polym Sci 2006, 102, 3691.

13. Ke, Y. C.; Long, C. F.; Qi, Z. N. J Appl Polym Sci 1999, 71, 1139.
14. Mun, M. K.; Kim, J. C.; Chang, J. H. Polym Bull 2006, 57, 797.
15. Guan, G. H.; Li, C. C.; Zhang, D. J Appl Polym Sci 2005, 95, 1443.
16. Di Lorenzo, M. L.; Errico, M. E.; Avella, M. J. Mater Sci 2002, 37, 2351.
17. Tzavalas, S.; Drakonakis, V.; Mouzakis, D. E.; Fischer, D.; Gregoriou, V. G. Macromolecules 2006, 39, 9150.
18. Neaman, A.; Singer, A. Appl Clay Sci 2004, 25, 121.
19. Augsburger, M. S.; Strasser, E.; Perino, E.; Mercader, R. C.; Pedregosa, J. C. J Phys Chem Solids 1998, 59, 175.
20. Murray, H. H. Appl Clay Sci 2000, 17, 207.
21. Wang, L. H.; Sheng, J. Polymer 2005, 46, 6243.
22. Li, A.; Wang, A. Q.; Chen, J. M. J Appl Polym Sci 2004, 92, 1596.
23. Zhang, J. P.; Chen, H.; Li, P.; Wang, A. Q. Macromol Mater Eng 2006, 291, 1529.
24. Shen, L.; Lin, Y. J.; Du, Q. G.; Zhong, W. Compos Sci Technol 2006, 66, 2242.
25. Pan, B. L.; Yue, Q. F.; Ren, J. F.; Wang, H. G.; Jian, L. Q.; Zhang, J. Y.; Yang, S. R. Polym Test 2006, 25, 384.
26. Xue, S. Q.; Reinholdt, M.; Pinnavaia, T. J. Polymer 2006, 47, 3344.
27. Lu, H. B.; Shen, H. B.; Song, Z. L.; Shing, K. S.; Tao, W.; Nutt, S. Macromol Rapid Commun 2005, 26, 1445.
28. Rong, J. F.; Sheng, M.; Li, H. Q.; Ruckenstein, E. Polym Compos 2002, 23, 658.
29. Lai, S. Q.; Li, T. S.; Liu, X. J.; Lv, R. G.; Yue, L. Tribol Int 2006, 39, 541.
30. Ni, P.; Li, J.; Suo, J. S.; Li, S. B. J Mater Sci 2004, 39, 4671.
31. Lai, S. Q.; Yue, L.; Li, T. S.; Liu, X. J.; Lv, R. G. Macromol Mater Eng 2005, 290, 195.
32. Tian, M.; Qu, C. D.; Feng, Y. X.; Zhang, L. Q. J Mater Sci 2003, 38, 4917.
33. Chen, X. Q.; Xu, J. J.; Lu, H. B.; Yang, Y. L. J Polym Sci Part B: Polym Phys 2006, 44, 2112.
34. Yuan, X. P.; Li, C. C.; Guan, G. H.; Liu, X. Q.; Mao, Y. N.; Zhang, D. J Appl Polym Sci 2007, 103, 1279.
35. Bikiaris, D.; Karavelidis, V.; Karayannidis, G. Macromol Rapid Commun 2006, 27, 1199.
36. Laible, R.; Hamann, K. Adv Colloid Interface Sci 1980, 13, 65.
37. Wan, T.; Chen, L.; Chua, Y. C.; Lu, X. H. J Appl Polym Sci 2004, 94, 1381.
38. Chan, C. M.; Wu, J. S.; Li, J. X.; Cheung, Y. K. Polymer 2002, 43, 2981.
39. Wang, L. H.; Sheng, J. J Macromol Sci Phys 2006, 45, 1.
40. Armeniades, C. D.; Baer, E. J Polym Sci Part A-2: Polym Phys 1971, 9, 1345.
41. Chen, L. P.; Yee, A. F.; Goetz, J. M.; Schaefer, J. Macromolecules 1998, 31, 5371.
42. Maxwell, A. S.; Monnerie, L.; Ward, I. M. Polymer 1998, 39, 6851.
43. Illers, K. H.; Breuer, H. J Colloid Sci 1963, 18, 1.
44. Xia, Z. Y.; Sue, H. J.; Hsieh, A. J.; Huang, J. W. L. J Polym Sci Part B: Polym Phys 2001, 39, 1394.
45. Savin, D. A.; Pyun, J.; Patterson, G. D.; Kowalewski, T.; Matyjaszewski, K. J Polym Sci Part B: Polym Phys 2002, 40, 2667.
46. Zhao, B.; Zhu, L. J Am Chem Soc 2006, 128, 4574.